Inorg. Chem. **2003**, *42*, 2894–2901

Tetramethylphosphonium Fluoride: "Naked" Fluoride and Phosphorane

Andreas Kornath* and F. Neumann

Anorganische Chemie, Fachbereich Chemie der Universität Dortmund, D-44221 Dortmund, Germany

H. Oberhammer

Institut für Physikalische und Theoretische Chemie, Universität Tübingen, D-72076 Tübingen, Germany

Received November 8, 2002

Me_4PF was investigated in the solid state, in the gas phase, and in solutions. Vibrational spectra of the solid and a single-crystal structure show an ionic tetramethylphosphonium fluoride. The compound crystallizes in the space group *Pbca* with $a = 1016.0(1)$, $b = 1018.0(1)$, $c = 1205.8(4)$ pm, and $Z = 8$. The fluoride ion is nearly trigonal planar surrounded by three Me_4P^+ cations forming six H···F contacts between 218 and 240 pm. The compound is stable below 120 °C and sublimes in a vacuum. It possesses a phosphorane structure in the gas phase that was studied by electron diffraction and vibrational spectra, and additionally by theoretical calculations. The Me_4PF molecule has a trigonal bipyramidal structure with one methyl group and the fluorine atom in axial positions and bond lengths of $d(PC_{eq}) = 182.6(4)$ pm, $d(PC_{ax}) = 188.4(8)$ pm, and $d(PF) = 175.3(6)$ pm. The compound is remarkably soluble in acetonitrile, water, and alcohols, and slightly soluble in benzene, dimethyl ether, and diethyl ether. The solutions were studied by ^1H, ^{13}C, ^{19}F, and ^{31}P NMR spectroscopy. The hygroscopic Me_4PF forms a tetrahydrate which crytallizes in the space group $I4_1/a$ with $a = 1106.1(1)$ pm, $c = 816.3(1)$ pm, and $Z = 4$. The fluoride ion in $Me_4PF \cdot 4\ H_2O$ is surrounded by four water molecules. These units form a three-dimensional network in which the Me_4P^+ cations are embedded without any contacts.

Introduction

In the past decade a number of compounds have been reported that serve as sources for the so-called "naked" fluoride. At first, Christe et al. reported a procedure for the preparation of anhydrous Me_4NF.[1] Later, several novel anions have been prepared with naked fluorides.[2−10] These examples demonstrate a higher reactivity of the fluoride ion in Me_4NF compared to alkali-metal fluorides. The unusual reactivity was explained by Seppelt with the cesium effect.[11] It is well-known that in the series of alkali-metal fluorides the reactivity of the fluoride ion increases with the size of the counterion, thus CsF displays the highest reactivity as a consequence of an unfavorable ratio of the ion sizes in the crystal lattice. Consequently, several anhydrous fluorides with larger organic cations than Me_4N^+ have been described with the aim of obtaining a more naked fluoride.[12−16] However, it has not

* Author to whom correspondence should be addressed. E-mail: kornath@citrin.chemie.uni-dortmund.de.

(1) Christe, K. O.; Wilson, W. W.; Wilson, R. D.; Bau, R.; Feng, J. *J. Am. Chem. Soc.* **1990**, *112*, 7619.
(2) Christe, K. O.; Wilson, W. W.; Chirakal, R. V.; Sanders, J. C. P.; Schrobilgen, G. J. *Inorg. Chem.* **1990**, *29*, 3506.
(3) Christe, K. O.; Sanders, J. C. P.; Schrobilgen, G. J.; Wilson, W. W. *J. Chem., Chem. Commun.* **1991**, 837.
(4) Mahjoub, A.-R.; Seppelt, K. *J. Chem. Soc., Chem. Commun.* **1991**, 840.
(5) Christe, K. O.; Dixon, D. A.; Mahjoub, A. R.; Mercier, H. P. A.; Sanders, J. C. P.; Seppelt, K.; Schrobilgen, G. J.; Wilson, W. W. *J. Am. Chem. Soc.* **1993**, *115*, 2696.
(6) Christe, K. O.; Dixon, D. A.; Sanders, J. C. P.; Schrobilgen, G. J.; Wilson, W. W. *Inorg. Chem.* **1993**, *32*, 4089.
(7) Christe, K. O.; Dixon, D. A.; Mercier, H. P. A.; Sanders, J. C. P.; Schrobilgen, G. J.; Wilson, W. W. *J. Am. Chem. Soc.* **1994**, *116*, 2850.
(8) Zhang, X.; Gro*β*, U.; Seppelt, K. *Angew. Chem.* **1995**, *107*, 2019; *Angew. Chem., Int. Ed. Engl.* **1995**, *34*, 1858.
(9) Drake, G. W.; Dixon, D. A.; Sheehy, J. A.; Boatz, J. A.; Christe, K. O. *J. Am. Chem. Soc.* **1998**, *120*, 8392.
(10) Kornath, A.; Kadzimirsz, D.; Ludwig, R. *Inorg. Chem.* **1999**, *38*, 3066.
(11) Seppelt, K. *Angew. Chem.* **1992**, *104*, 299; *Angew. Chem., Int. Ed. Engl.* **1992**, *31*, 292.
(12) Schwesinger, R.; Link, R.; Thiele, G.; Rotter, H.; Honert, D.; Limbach, H.-H.; Männle, F. *Angew. Chem.* **1991**, *103*, 1376; *Angew. Chem., Int. Ed. Engl.* **1991**, *30*, 1372.
(13) Harmon, K. M.; Southworth, B. A.; Wilson, K. E.; Keefer, P. K. *J. Org. Chem.* **1993**, *58*, 7294.

10.1021/ic020663c CCC: $25.00
Published on Web 04/09/2003

been demonstrated that these compounds serve as better sources for the naked fluoride than Me_4NF. Another explanation for the reactivity of the naked fluoride ion sources is their solubility in aprotic solvents such as acetonitrile or THF. At least Grushnin reported an in situ method for anhydrous fluoride solutions.[17] The nakedness of the fluoride ion in solutions should depend rather upon the solvent than the counterion. Comparison of different naked fluoride ion sources is difficult because of the lack of a suitable scale. The influences of the counterions, and the solvent, are not well understood.

In 1972 Schmidbaur et al. reported the synthesis of Me_4PF.[18] The properties of the compound did not fit into the series of the known phosphoranes Me_nPF_{5-n} ($n = 1-3$). The solid did not melt below 100 °C in a glass tube. The experimental results indicated an ionic composition in the solid, but in contrast to $Me_4P^+Cl^-$ also a vapor pressure already at room temperature was found. Despite these surprising properties, no further investigations have been reported. These findings were interesting to us in the course of our studies, as Me_4PF should serve as a naked fluoride source with unique properties due to its volatility. We report herein studies of Me_4PF in the solid state, in the gas phase, and in solutions.

Experimental Section

Apparatus and Materials. All synthetic work and sample handling were performed employing standard Schlenk techniques and a standard vacuum line. Organic solvents were dried by standard methods. KHF_2 was dried at 120 °C.

Caution! Trimethylphosphine is pyrophoric in air. The toxicities of trimethylmethylidenphosphorane and tetramethylphosphonium fluoride are not known.

Infrared spectra were recorded on a Bruker IFS 113v spectrophotometer. Spectra of dry powders were obtained using a CsBr plate coated with the neat sample. The gas-phase spectrum of Me_4PF was measured with a heated cell at 60 °C. The Raman spectra were recorded on an ISA T64000 using an Ar^+ laser tube (514.5 nm) from Spectra Physics. The spectra of the solids were recorded in a glass cell cooled with liquid nitrogen. For gaseous Me_4PF a heated quartz cell (+100 °C) was used. The NMR spectra were recorded with a Bruker DPX 300 spectrometer. Single crystals were placed in Lindemann capillaries in a cooled stream of nitrogen, and the X-ray diffraction studies were carried out using an ENRAF Nonius Kappa CCD diffractometer.

Synthesis of Me_3P. The synthesis was carried out as described in ref 19 from MeMgI and $(PhO)_3P$, but with substitution of diethyl ether by dibutyl ether to avoid the complicated diethyl ether/Me_3P separation. The product was distilled from the reaction mixture with a bath temperature up to 160 °C through a Vigreux column with a yield of 77%. Further purification of the colorless liquid (bp: 38 °C) is not necessary.

Synthesis of Me_4PBr. In a 250-mL glass vessel with a grease-free valve, ca. 130 mL of abs. diethyl ether, 7.61 g (0.1 mol) of Me_3P, and 10.4 g (0.11 mol) of methyl bromide were condensed at −196 °C. The frozen mixture was warmed to room temperature and stirred for 1 day. The volatiles were removed in dynamic vacuum. The remaining white microcrystalline powder consisted of pure tetramethylphosphonium bromide which was formed in an almost quantitative yield.

Synthesis of $Me_3P{=}CH_2$. The synthesis was carried out as described in ref 20 from $Me_4P^+Br^-$ and $NaNH_2$ in THF with modification of the purification procedure. Almost all of the THF is distilled from the resulting reaction mixture through a short glass column. The residue is slowly condensed in a dynamic vacuum through a trap cooled to −40 °C, where the pure product crystallizes with a yield of 90%. The colorless liquid (mp +11 °C; bp 122 °C) is extremely moisture- and air-sensitive.

Synthesis of Me_4PF. Dried KHF_2 (10.1 g; 0.13 mol) and 50 mL of dried THF were placed in a 100-mL glass vessel with a grease-free valve, and 9.0 g (0.1 mol) of $Me_3P{=}CH_2$ were condensed at −196 °C. The frozen mixture was warmed to room temperature and stirred for 1 day. After removal of the solvent in dynamic vacuum at −30 °C, the product was sublimed at 35 °C from the white residual solid in a dynamic vacuum onto a coldfinger (−196 °C) with a yield of 8.0 g (73%). The colorless, crystalline, and extremely hygroscopic Me_4PF is stable in a dry glass ampule up to 120 °C. At higher temperatures, the glass is etched under formation of various volatile products and Me_3PO.

The sublimation pressure was measured in the range of 20−100 °C using a calibrated pressure gauge (MKS). A logarithmic plot of the pressure versus the reciprocal temperature yields a linear correlation according to the equation: $\ln(p/[hPa] = 21.11 - 6053K/T$, sublimation enthalpy ($\Delta_sH°$) of 50.2 kJ/mol, sublimation entropy ($\Delta_sS°$) of 117 J/molK, and an extrapolated sublimation point of 153 °C. Suitable crystals for X-ray diffraction studies were obtained by sublimation. Crystals of $Me_4PF^-{\cdot}4\ H_2O$ were obtained by crystallization of Me_4PF from slightly wet acetonitrile.

Computational Methods. The ab initio calculations for Me_4PF were performed at different levels of theory by using the Hartree−Fock (HF) method,[21] the second-order Møeller−Plesset perturbation theory (MP2),[22,23] and the density functional theory (DFT) method B3LYP.[24] As basis sets we have chosen 3-21G*, 6-31G*, 6-31+G*, 6-311G**, and 6-311G(2df). The methods used and the basis sets are all implemented in the Gaussian 94 Program.[25]

Gas-Phase Structure of Me_4PF. The electron diffraction intensities were recorded with a Eldigraph KDG-2 at the University of Oslo at 25 and 50 cm nozzle-to-plate distances and with an

(14) Bennett, B. K.; Harrison, R. G.; Richmond, T. G. *J. Am. Chem. Soc.* **1994**, *116*, 11165.
(15) Mahjoub, A. R.; Zhang, X.; Seppelt, K. *Chem. Eur. J.* **1995**, *1*, 261.
(16) Gnann, R. Z.; Wagner, R. I.; Christe, K. O.; Bau, R.; Olah, G. A.; Wilson, W. W. *J. Am. Chem. Soc.* **1997**, *119*, 112.
(17) Grushin, V. V. *Angew. Chem.* **1998**, *110*, 1042; *Angew. Chem., Int. Ed.* **1998**, *37*, 994.
(18) Schmidbaur, H.; Mitschke, K.-H.; Weidlein, J. *Angew. Chem.* **1972**, *84*, 165. Schmidbaur, H.; Mitschke, K.-H.; Buchner, W.; Stühler, H.; Weidlein, J. *Chem. Ber.* **1973**, *106*, 1226.
(19) Wolfsberger, W.; Schmidbaur, H. *Synth. React. Inorg. Met.−Org. Chem.* **1974**, *4*, 149.
(20) Klein, H. F. *Inorg. Synth.* **1978**, *18*, 139.
(21) Hehre, W. G.; Radom, L.; Schleyer, P. v.; Pople, J. A. *Ab initio Molecular Orbital Theory*; Wiley: New York, 1986.
(22) Møeller, C.; Plesset, M. S. *Phys. Rev.* **1934**, *46*, 618.
(23) Head-Gordon, M.; Pople, J. A.; Frisch, M. J. *Chem. Phys. Lett.* **1988**, *153*, 503.
(24) Becke, A. D. *J. Chem. Phys.* **1996**, *104*, 1040.
(25) GAUSSIAN 94 (Revision A.1) Frisch, J. M.; Trucks, G. W.; Schlegel, H. B.; Gill, P. M. W.; Johnson, B. G.; Robb, M. A.; Cheeseman, J. R.; Keith, T.; Petersson, G. A.; Montgomery, J. A.; Raghavachari, K.; Al-Laham, M. A.; Zakrzewsky, V. G.; Ortiz, J. V.; Foresman, J. B.; Cioslowski, J.; Stefanov, B. B.; Nanayakkara, A.; Challacombe, M.; Peng, C. Y.; Ayala, P. Y.; Chen, W.; Wong, M. W.; Andres, J. L.; Replogle, E. S.; Gomperts, R.; Martin, R. L.; Fox, D. J.; Binkley, J. S.; Defrees, D. J.; Baker, J.; Stewart, J. P.; Head-Gordon, M.; Gonzalez, C.; Pople, J. A. Gaussian, Inc.: Pittsburgh, PA, 1995.

accelerating voltage of ca. 60 kV.[26] The sample and the nozzle were heated to 70 °C. The photographic plates (Kodak Electron Image Plates 18 × 13 cm) were analyzed with the usual methods.[27] Averaged molecular intensities in the *s* ranges 20−180 and 30−350 nm^{-1} in steps of $\Delta s = 2$ nm^{-1} were used for the structure analysis.

Results and Discussion

Synthesis and Properties of Me_4PF. The salt was prepared in an overall yield of 50% in a four-step synthesis according to the following sequence (Formula 1):

$$P(OPh)_3 \xrightarrow[77\%]{MeMgBr} Me_3P \xrightarrow[98\%]{MeBr} Me_4P^+Br^- \xrightarrow[90\%]{NaNH_2} Me_3P{=}CH_2 \xrightarrow[73\%]{KHF_2} Me_4P^+F^-$$

The key step of the synthesis is the addition of hydrogen fluoride to the P═C bond which can be carried out with pure anhydrous HF. A more convenient method is the use of KHF_2. The resulting Me_4PF is separated from KF/KHF_2 by sublimation at 35 °C.

Me_4PF is a colorless salt, stable up to 120 °C in glass vessels. The glass is etched at higher temperatures under formation of various volatile products and Me_3PO. Tetramethylphosphonium fluoride does not melt below 120 °C, but it has a vapor pressure according to the equation $\ln(p/[hPa]) = 21.11 - 6053K/T$ with an extrapolated sublimation point of 153 °C. These properties are in contrast to the known tetramethylphosphonium salts of the heavier halides, which decompose in the region of 300 °C and do not sublime. The gas-phase of the salt was characterized by vibrational spectroscopy and electron diffraction which are discussed later.

Me_4PF fumes in air, absorbing moisture under formation of various hydrates, of which the tetrahydrate has been characterized by single-crystal X-ray diffraction. The tetrahydrate is stable in a vacuum up to 90 °C. At higher temperatures decomposition under formation of Me_3PO, $Me_4P^+HF_2^-$, and various volatile products takes place. The removal of water, as used for the preparation of anhydrous Me_4NF, is not possible, but Me_4PF containing only small amounts of water can be separated from the hydrates by vacuum sublimation at ambient temperatures. The Me_4PF is highly soluble in water, methanol, and ethanol. The solubility in acetonitrile is remarkably high (0.7 mol/L) compared to the concentration of 56 mmol/L reached by the in situ method of Grushnin in dichloromethane.[17] It should be noted that such solutions in dichloromethane are useless for chemical reactions because the fluoride ion reacts quickly with the solvent. Acetonitrile solutions are stable at room temperature for a limited time and decompose in a way similar to that described for Me_4NF, due to a proton abstraction from CH_3CN by the fluoride ion. Me_4PF is also slightly soluble in solvents such as THF, benzene, diethyl ether, and dimethyl ether. It reacts with dichloromethane immediately under chlorine−fluorine exchange. With sulfur dioxide an exothermic reaction under formation of $Me_4P^+SO_2F^-$ takes place.

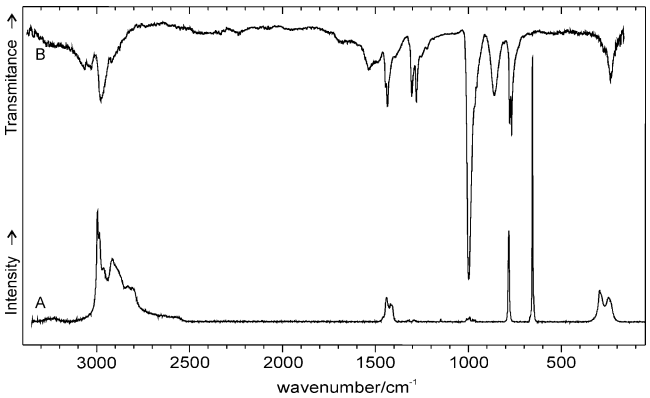

Figure 1. Raman spectrum (trace A) and infrared spectrum (trace B) of solid Me_4PF.

Vibrational Spectra of Solid Me_4PF. The infrared and Raman spectrum of solid Me_4PF are shown in Figure 1 and the observed frequencies are summarized in Table 1. In accordance with a crystal structure, which is discussed later, comparison of the vibrational spectra with those of $Me_4P^+Br^-$ show an ionic composition of the solid with a tetrahedral Me_4P^+ ion. Consequently, 19 fundamental vibrations ($3A_1 + A_2 + 4E + 4F_1 + 7F_2$) are expected. Species A_1, E, and F_2 are Raman active and only species F_2 is infrared active. For both salts in Table 1 more vibrations are observed than expected by the selection rules. This is due to crystal field splitting as well as interactions between cations and anions in the crystal lattice which lead to a slight distortion of the T_d symmetry. Nevertheless, the assignments for Me_4P^+ were made according to a tetrahedral symmetry for both salts. The stretching and deformation modes of the methyl group are observed in their typical regions and comparable to those observed for the Me_4N^+ cation.[1] The four modes of the PC_4 skeleton occur below 800 cm^{-1}. The symmetric and only Raman active PC stretching mode occurs at 656 cm^{-1}.

Crystal Structure of Me_4PF and $Me_4PF \cdot 4\ H_2O$. The crystal data are summarized in Table 2. The Me_4PF crystallizes in the orthorhombic space group *Pbca* with 8 formula units per unit cell, and $Me_4PF \cdot 4\ H_2O$ crystallizes in the tetragonal space group $I4_1/a$ with four formula units per unit cell. For the data reduction, structure solution, and refinement, SCALE PACK, programs in the SHELXTL package, and PARST were used.[28−31] The phosphorus layers were found by the Patterson method. All atoms including protons were found in the difference Fourier synthesis, and a final refinement with anisotropic (except for H atoms) thermal parameters gave *R* values of 0.025 for Me_4PF and 0.026 for $Me_4PF \cdot 4\ H_2O$.[32]

(26) Oberhammer, H. *Molecular Structures by Diffraction Methods*; The Chemical Society: London, 1976; Vol. 4, p 24.
(27) Oberhammer, H.; Gombler, W.; Willner, H. *J. Mol. Struct.* **1981**, *70*, 273.
(28) Otwinowski, Z.; Minor, W. *Methods Enzymol.* **1997**, *276*, 307.
(29) Sheldrick, G. M. *SHELXTL PLUS An Integrated System for Solving, Refining, and Displaying Structures from Diffraction Data*; University of Göttingen: Germany, 1987.
(30) Sheldrick, G. M. *SHELXL 93*; Universität Göttingen: Germany, 1993.
(31) Nardelli, M. *Comput. Chem.* **1993**, *7*, 95.
(32) More details about the crystal structure are available at the Fachinformationzentrum Karlsruhe, Gesellschaft für Wissenschaftlich-Technische Information mbH, D-76344 Eggenstein-Leopoldshafen.

Table 1. Vibrational Frequencies (cm^{-1}) of Solid $Me_4P^+F^-$ and $Me_4P^+Br^-$

$Me_4P^+F^-$		$Me_4P^+Br^-$		assignments	
IR	Raman	IR	Raman		
3048 w					
3017 w	2996 (38)		3004 (25)	ν_{13} (F_2)	$\nu_{as}(CH_3)$
	2985 (28)			ν_5 (E)	$\nu_{as}(CH_3)$
2964 ms	2964 (31)	2964 m			
2909 m	2916 (100)		2926 (100)	ν_1 (A_1)	$\nu_s(CH_3)$
2868 w		2873 vw		ν_{14} (F_2)	$\nu_s(CH_3)$
	2833 (23)	2854 vw	2852 (2)		
	2809 (30)		2803 (5)		
1539 m, br				$2\nu_{18}$ (F_2)	
1451 m	1460 (1)	1414 w		ν_{15} (F_2)	$\delta_{as}(CH_3)$
1440 m	1442 (12)		1412 (12)	ν_6 (E)	$\delta_{as}(CH_3)$
	1419 (4)				
	1412 (5)			ν_2 (A_1)	$\delta_s(CH_3)$
1312 m	1326 (0.4)	1288 m	1333 (0.5)	ν_{16} (F_2)	$\delta_s(CH_3)$
1286 m	1292 (0.7)		1308 (0.5)		
1006 s	1010 (1)	991 vs	987 (1)	ν_{17} (F_2)	$\rho(CH_3)$
976 sh	999 (1)				
	977 (0.6)		946 (1)	ν_7 (E)	$\rho(CH_3)$
	966 (0.4)				
871 m					
791 s	782 (19)	774 m	779 (10)	ν_{18} (F_2)	ν_{as} (C_4P)
778 s					
	656 (33)		648 (65)	ν_3 (A_1)	ν_s (C_4P)
293 m	294 (26)	276 m	286 (14)	ν_{19} (F_2)	$\delta_{as}(C_4P)$
255 m	247 (22)		243 (13)	ν_8 (E)	$\delta_s(C_4P)$

Table 2. Crystallographic Data of Me_4PF and $Me_4PF{\cdot}4H_2O$

formula	Me_4PF	$Me_4PF{\cdot}4\ H_2O$
formula weight, g mol^{-1}	110.11	182.17
temperature, °C	−116(2)	20 (2)
space group	*Pbca* (No. 61)	$I4_1/a$ (No. 88)
Z	8	4
a, pm	1016.0(1)	1106.1 (1)
b, pm	1018.0(1)	1106.1 (1)
c, pm	1205.8(4)	816.3 (1)
V, 10^6 pm^3	1247.1(2)	998.7 (2)
density calcd., g cm^{-3}	1.173	1.212
μ, cm^{-1}	0.7305	2.60
λ, pm	71.069	71.069
GOF on F^2	1.098	0.857
R[a] [$I > 2\sigma(I)$]	R1 = 0.0250	R1 = 0.0257
	wR2 = 0.0722	wR2 = 0.0510
R[a] (all data)	R1 = 0.0295	R1 = 0.0679
	wR2 = 0.0738	wR2 = 0.0551
largest diff peak and hole	0.245 and	0.146 and
	−0.261 e · 10^6 pm^3	−0.200 e · 10^6 pm^3

[a] $R = \sum||F_o| - |F_c||/\sum|F_o|$; Refinement: full-matrix least-squares on F^2.

Table 3. Selected Bond Distances (pm) and Angles (°) of $Me_4P^+F^-$

P(1)−C(1)	177.18(12)	C(1)−P(1)−C(2)	109.29(7)
P(1)−C(2)	178.31(13)	C(1)−P(1)−C(3)	108.88(7)
P(1)−C(3)	177.56(13)	C(1)−P(1)−C(4)	111.51(7)
P(1)−C(4)	178.31(13)	C(2)−P(1)−C(3)	110.00(8)
F(1)···H(11)	221.2(15)	C(2)−P(1)−C(4)	110.18(7)
F(1)···H(22)	226.7(18)	C(3)−P(1)−C(4)	106.93(7)
F(1)···H(32a)[a]	240.3(15)		
F(1)···H(43a)	218.3(18)		
F(1)···H(12b)	219.1(14)		
F(1)···H(33b)	236.3(18)		

[a] Symmetry transformations: (a) 0.5 − *x*, 0.5 + *y*, *z*; (b) −*x*, 0.5 + *y*, 0.5 − *z*.

Bond lengths and selected angles of Me_4PF are summarized in Table 3. The lengths of the P−C bonds and the C−P−C angles show only small deviations from an ideal tetrahedral geometry and are in good agreement with known Me_4P^+ salts.[33] Each fluoride ion and the P atoms of three

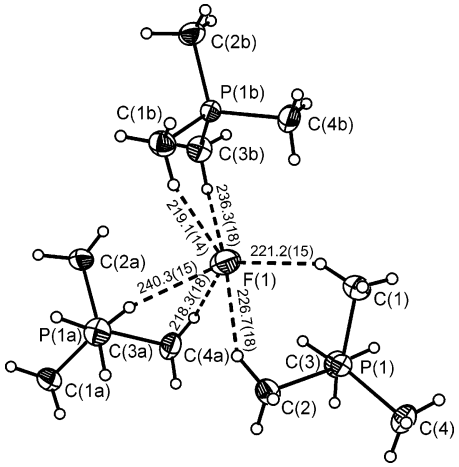

Figure 2. Environment of the fluoride in Me_4PF showing the 50% probability displacement ellipsoids. Symmetry transformations: (a) 0.5 − *x*, 0.5 + *y*, *z*; (b) −*x*, 0.5 + *y*, 0.5 − *z*.

surrounding Me_4P^+ cations form nearly planar structures with six H···F interactions, that are less than the sum of the van der Waals radii (267 pm)[34] ranging from 218.3 to 240.3 pm (Figure 2). The Me_4P^+ cations are staggered along the *b* axis in the crystal and linked via the secondary H···F interactions to two-dimensional networks in the *ab* plane.

Crystal structures of two naked fluoride sources are known in the literature. In hexamethylpiperidinium fluoride (PIPF) seven H···F contacts between 196 and 247 pm were found; the diphosphazenium salt $\{[Me_2N]_3P{=}N{=}P[NMe_2]_3\}^+F^-$ shows six H···F contacts of 237 and 257 pm, respectively.[12,15] Following the cesium effect, both salts should serve as better fluoride ion donors than Me_4PF due to their larger size. In general, coordination of the fluoride ion by hydrogen contacts

(33) Allen, F. H.; Kennard, O.; Watson, D. G.; Brammer, L.; Orpen, A. G.; Taylor, R. *J. Chem. Soc., Perkin Trans. 2* **1987**, 1.
(34) Bondi, A. *J. Phys. Chem.* **1964**, *68*, 441.

Table 4. Selected Bond Distances (pm) and Angles (°) of $Me_4P^+F^-\cdot 4H_2O$

P(1)−C(1)	177.55(12)	C(1)−P(1)−C(1a)[a]	109.35(11)
O(1)−H(4)	77(2)	C(1)−P(1)−C(1b)	109.53(5)
O(1)−H(5)	82(2)	H(4)−O(1)−H(5)	114(2)
F(1)···H(4c)	189	F(1)···H(4c)−O(1d)	177
F(1)···O(1d)	266	O(1)−H(5)···O(1d)	178
O(1c)···H(5)	200		
O(1)···O(1d)	282		

[a] Symmetry transformations: (a) $-x$, $0.5 - y$, z; (b) $-0.25 + y$, $0.25 - x$, $0.25 - z$; (c) $0.25 - y$, $0.25 + x$, $0.25 - z$; (d) $0.5 - x$, $-y$, $0.5 + z$.

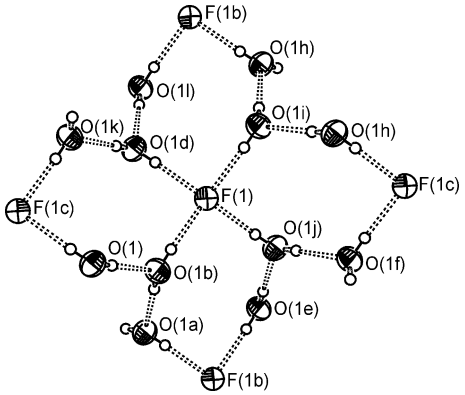

Figure 3. Environment of the fluoride in $Me_4PF\cdot 4\ H_2O$ showing the 50% probability displacement ellipsoids. Symmetry transformations: (a) $0.75 - y$, $0.25 + x$, $0.25 + z$; (b) $0.5 - x$, $-y$, $0.5 + z$; (c) $0.75 + y$, $0.75 - x$, $0.75 + z$; (d) $-x$, $-y$, $-z$; (e) $0.5 + x$, y, $0.5 - z$; (f) $0.25 - y$, $0.25 + x$, $0.25 - z$; (g) $0.5 + x$, $0.5 + y$, $0.5 + z$; (h) $0.25 - y$, $0.75 + x$, $0.75 + z$; (i) $0.25 + y$, $0.25 - x$, $0.25 + z$; (j) $0.75 + y$, $0.25 - x$, $0.25 - z$; (k) x, $0.5 + y$, $-z$; (l) $0.75 - y$, $0.75 + x$, $0.75 - z$.

decreases the nakedness of the fluoride ion to some extent, especially when molecules such as water or HF are involved. In the tetrahydrates $Me_4PF\cdot 4\ H_2O$ and $Me_4NF\cdot 4\ H_2O$ the fluoride ion is surrounded by four water molecules with H···F contacts of 189 and 174 pm, respectively,[35] and the HF_2^- ion with short H−F distances of 110.7 pm can be seen as a counterpart for a naked ion.[36]

Bond lengths and selected angles of $Me_4PF\cdot 4\ H_2O$ are summarized in Table 4. The lengths of the P−C bonds and the C−P−C angles show an ideal tetrahedral geometry and are in good agreement with known Me_4P^+ cations.[33] The fluoride ions are surrounded by four water molecules with H···F distances of 189 pm (O−(H)···F distances 266 pm) in an arrangement that is closer to square planar than to tetrahedral. Further condensation of such units via hydrogen bridging (O−H···O) results in a buckled network of chair-shaped hexagons (Figure 3). The Me_4P^+ cations lie at the intersections of buckled channels which are formed by the hydrogen-bonded nets and extend in the *a* and *b* axial directions (Figure 4). This framework structure is similar to that of $Me_4NF\cdot 4\ H_2O$.[35] The water molecules are three coordinated with two hydrogen bonds (O−(H)···O) of 282 pm and one (O−(H)···F) of 266 pm. The latter is in the range of that found in $Me_4NF\cdot 4\ H_2O$ (263 pm) and $KF\cdot 4\ H_2O$ (273 pm).[35,37] The cations are embedded in the framework

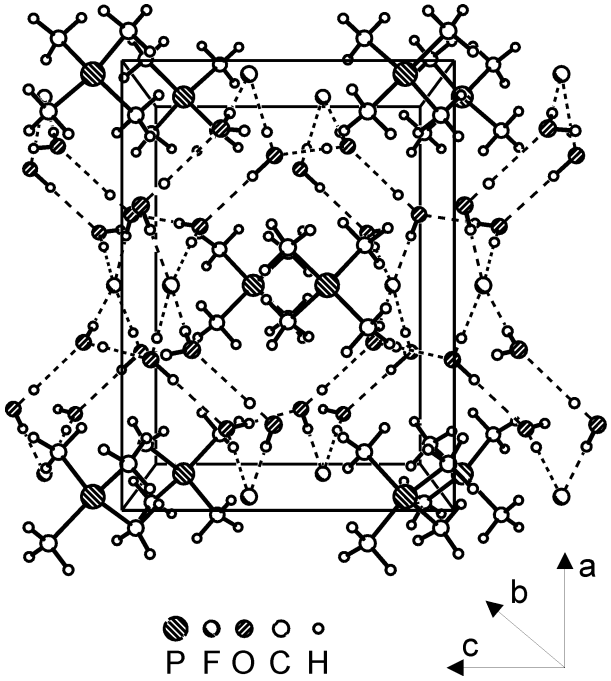

Figure 4. Projection of the structure of $Me_4PF\cdot 4\ H_2O$.

Table 5. Chemical Shifts (ppm) and Coupling Constants (Hz) of Me_4NF and Me_4PF in Different Solvents

	Me_4NF	Me_4PF					
solvent	^{19}F	^{19}F	^{1}H	^{13}C	^{31}P	$^{1}J_{PC}$	$^{2}J_{PH}$
water	−119	−119	1.9	8.3	23.1	57	15
methanol	−147	−149	2.1	9.0	25.5	56	15
ethanol	−137	−134	2.0	9.3	25.2	56	15
acetonitrile	−71	−70		9.0	24.8	56	15
diethyl ether		+51		20.1	29.5	69	13
dimethyl ether		+51	1.5	18.1	31.3	70	13
tetrahydrofuran		+49	1.4	18.6	31.3	69	13
benzene		+48	1.4	17.9	30.7	69	13

structure without any contacts below the sum of the van der Waals radii.

NMR Spectroscopy of Me_4PF. The NMR data of Me_4PF in different solvents are summarized in Table 5. The ^1H, ^{13}C, and ^{31}P NMR chemical shifts and coupling constants of Me_4PF dissolved in water, methanol, ethanol, and acetonitrile are typical for the Me_4P^+ cation.[38−42] The ^{19}F NMR spectra show strongly solvent-dependent chemical shifts of the fluoride ion in the region between −70 and −149 ppm. Earlier investigations by Christe have shown that the wide range of the chemical shift is characteristic for the fluoride ion.[43] For each solvent the chemical shifts of Me_4PF are almost identical with those of Me_4NF and are not affected strongly by the counterion. This is supported by the comparison of the chemical shifts in Figure 5 for solutions in methanol, ethanol, and water (KF and CsF are not soluble in acetonitrile and dichloromethane). These examples show

(35) McLean, W. J.; Jeffrey, G. A. *J. Chem. Phys.* **1967**, *47*, 414.
(36) Wilson, W. W.; Christe, K. O.; Feng, J. A.; Bau, R. *Can. J. Chem.* **1989**, *67*, 1898.
(37) Beurskens, G.; Jeffrey, G. A. *J. Chem. Phys.* **1964**, *41*, 917.
(38) Elser, H.; Dreeskamp, H. *Ber. Bunsen-Ges. Phys. Chem.* **1969**, *6*, 619.
(39) Karsch, H. H. *Phosphorus Sulfur Relat. Elem.* **1982**, *12*, 217.
(40) Evans, D. J.; Leigh, G. J.; MacDonald, C. J. *J. Magn. Reson. Chem.* **1990**, *28*, 711.
(41) Krannich, L. K.; Kanjolia, R. K.; Watkins, C. L. *J. Magn. Reson. Chem.* **1987**, *25*, 320.
(42) Lorenz, J.; Fluck, E. *Z. Naturforsch., B: Chem. Sci* **1967**, *22b*, 1095.
(43) Christe, K. O.; Wilson, W. W. *J. Fluorine Chem.* **1990**, *46*, 339.

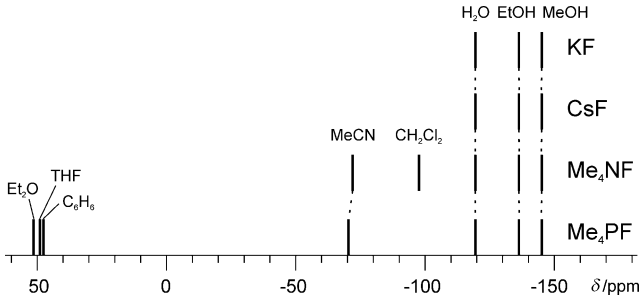

Figure 5. ^{19}F NMR shift of fluorides in different solvents.

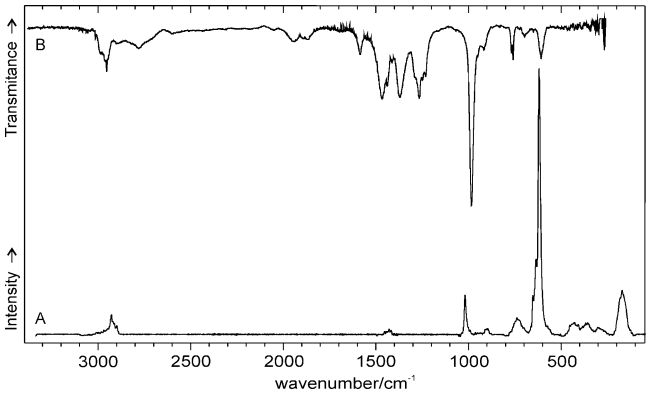

Figure 6. Raman spectrum (trace A) and infrared spectrum (trace B) of Me_4PF in the gas phase.

that the fluoride ion in solution is affected more strongly by the solvating sphere than by the counterion. The solvent dependency of the ^{19}F NMR shifts of the fluoride ion has been studied recently by theoretical calculations.[44] It has been shown that the ^{19}F NMR shift of the fluoride ion cannot be considered as a measure of its nakedness, because the large solvent dependency of the fluoride shifts is due to varying amounts of solvent-induced paramagnetic shielding and it does not correlate to the calculated binding energy between fluoride and the corresponding solvent molecules.

Me_4PF is slightly soluble in dimethyl ether, diethyl ether, THF, and benzene and shows different NMR spectra in these solvents. The ^{13}C and ^{31}P chemical shifts are outside the region of Me_4P^+ salts. The corresponding ^{19}F chemical shifts at around +50 ppm are in a region typical for alkylfluorophosphoranes.[18] This implies the assumption of a molecular form for Me_4PF in these solvents, however, in all NMR spectra a corresponding coupling with the fluorine atom is missing. A similar behavior is known for Et_4PF and Me_4SbF, both of which are known only in the molecular form.[18,45] The missing coupling was explained with fast exchange processes in solutions, and the relatively broad signals indicate that a similar exchange process can take place in Me_4PF.

Vibrational Spectra of Gaseous Me_4PF. The infrared and Raman spectra of gaseous Me_4PF are shown in Figure 6 and the observed frequencies are summarized in Table 6. An electron diffraction study and a DFT calculation, which are discussed later, yield a C_{3v} symmetry for the molecule. Consequently, 32 fundamental vibrations ($11A_1 + 5A_2 + 16E$) are expected, of which species A_1 and E are Raman and infrared active. The assignments were made by comparison with the calculated frequencies and consideration of the Cartesian displacement coordinates.

Table 6. Vibrational Frequencies (cm^{-1}) of Gaseous Fluorotetramethylphosphorane

exp.		B3LYP/6-31G* [a]			
IR	Raman	ν	IR−Int.	assignment	
3018 vw		3012	38.1	ν_1 (A_1)	$\nu_{as}(CH_3)_{eq}$
		3010	4.94	ν_{17} (E)	$\nu_{as}(CH_3)_{eq}$
2989 w		2997	7.93	ν_{18} (E)	$\nu_{as}(CH_3)_{eq}$
2955 m		2948	29.2	ν_{19} (E)	$\nu_{as}(CH_3)_{ax}$
	2939 (17)	2922	0.90	ν_2 (A_1)	$\nu_s(CH_3)_{eq}$
		2921	6.41	ν_{20} (E)	$\nu_s(CH_3)_{eq}$
		2873	10.4	ν_3 (A_1)	$\nu_s(CH_3)_{ax}$
2786 m					
1600 m					
1481 m					
1452 m		1436	0.15	ν_{21} (E)	$\delta_{as}(CH_3)$
	1436 (6.6)	1430	3.28	ν_{22} (E)	$\delta_{as}(CH_3)$
		1427	11.0	ν_4 (A_1)	$\delta_{as}(CH_3)_{eq}$
1386 m		1417	0.09	ν_{23} (E)	$\delta_{as}(CH_3)_{eq}$
1281 m		1311	0.04	ν_5 (A_1)	$\delta_s(CH_3)$
1264 m		1292	13.5	ν_{24} (E)	$\delta_s(CH_3)_{eq}$
1245 m		1278	16.3	ν_6 (A_1)	$\delta_s(CH_3)_{ax}$
999 vs	1027 (14)	976	96.2	ν_7 (A_1)	$\rho(CH_3)$
933 m		946	46.2	ν_{25} (E)	ρ (CH_3)
	904 (5)	907	32.9	ν_{26} (E)	ρ (CH_3)$_{eq}$
787 m		801	1.05	ν_{27} (E)	ρ (CH_3)
777 m					
717 w	727 (21)	698	15.2	ν_{28} (E)	$\nu_{as}(PC_3)_{eq}$
629 m	626 (100)	629	158	ν_8 (A_1)	$\nu(PC_{ax})$
	572 (17)	567	3.83	ν_9 (A_1)	$\nu_s(PC_3)_{eq}$
	435 (23)	462	21.4	ν_{10} (A_1)	ν(PF)
	362 (25)	358	18.4	ν_{29} (E)	$\delta(C_{eq}PF)$
		326	5.25	ν_{11} (A_1)	$\delta(PC_3)_{eq}$
	301 (21)	317	1.85	ν_{30} (E)	$\delta(C_{ax}PC_{eq})$
	176 (92)	161	1.46	ν_{31} (E)	$\delta(C_{eq}PC_{eq})$
		105	0.01	ν_{32} (E)	$\tau(CH_3)_{eq}$

[a] Scaled with an empirical factor 0.95; IR intensities in km/mol.

The stretching and deformation modes of the methyl groups are observed in their typical regions and comparable to that observed for Me_3PF_2.[46] The strongest infrared band at 999 cm^{-1} belongs to the rocking vibration of the equatorial methyl groups. It occurs for Me_3PF_2 at 1001 cm^{-1}. The stretching and deformation modes of the PC_4F skeleton are observed below 750 cm^{-1}. The $P-C_{ax}$ stretching mode at 626 cm^{-1} is the most intense line in the Raman spectrum. It occurs at lower wavenumbers than the mean value of the symmetric and antisymmetric $P-C_{eq}$ stretching mode, indicating a weaker $P-C_{ax}$ than $P-C_{eq}$ bond. The $P-F_{ax}$ stretching mode at 435 cm^{-1} is remarkably low. The vibrational frequencies of the $P-F_{ax}$ stretching modes decrease in the series of the known methylfluorophosphoranes with the number of methyl groups in the equatorial position (Table 7).[46−48] This trend goes along with a weakening of the $P-F_{ax}$ bond. In the case of Me_4PF an axial fluorine atom is formally substituted by a methyl group,

(44) Gerken, M.; Boatz, J. A.; Kornath, A.; Haiges, R.; Schneider, S.; Schroer, T.; Christe, K. O. *J. Fluorine Chem.* **2002**, *116*, 49.
(45) Schmidbaur, H.; Weidlein, J.; Mitschke, K.-H. *Chem. Ber.* **1969**, *102*, 4136.
(46) Downs, A. J.; Schmutzler, R. *Spectrochim. Acta* **1967**, *23A*, 681.
(47) Griffiths, J. E: Carter, R. P.; Holmes, R. R. *J. Chem. Phys.* **1964**, *41*, 863.
(48) Holmes, R. R.; Hora, C. J. *Inorg. Chem.* **1972**, *11*, 2506.

Table 7. Comparison of the P−F Stretching Vibrations of Methylfluorophosphoranes Me_nPF_{5-n} ($n = 0-4$)

PF_5 [a]	$MePF_4$ [b]	Me_2PF_3 [c]	Me_3PF_2 [c]	Me_4PF	assignments
1026	1009	}836			ν_{as} (PF_{eq})
817	932				ν_s (PF_{eq})
945	843	755	670	}435	ν_{as} (PF_{ax})
640	596	540	500		ν_s (PF_{ax})

[a] From Ref. 47. [b] From Ref. 48. [c] From Ref. 46.

Table 8. Comparison of Different Quantum Mechanical Methods for Fluorotetramethylphosphorane

method	basis set	d(P−F)	d(P−C_{eq})	d(P−C_{ax})
HF	3-21G*	169.5	182.6	189.2
	6-31G*	174.1	183.6	189.4
	6-31+G*	179.5	183.4	188.8
	6-311G**	179.9	183.0	188.5
	6-311G(2df)	172.9	182.8	188.7
MP2	6-31G*	176.2	183.6	188.8
	6-311G**	179.2	182.8	188.1
	6-311G(2df)	174.3	182.4	188.0
	cc-PVDZ	179.2	184.1	189.4
	cc-PVTZ	175.8	182.8	188.3
B3LYP	6-31G*	175.7	185.1	191.1
	6-311G**	182.0	184.3	190.2
	6-311G(2df)	176.6	183.9	189.8
exp.		175.3(6)	182.6(4)	188.4(8)

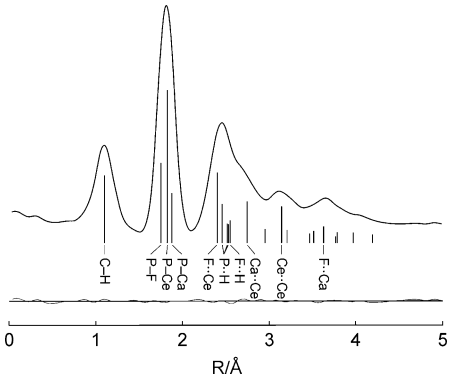

Figure 7. Experimental radial distribution function and difference curve. The positions of interatomic distances are indicated by vertical bars.

which obviously leads to an increased weakening of the P−F_{ax} bond. This is in accordance with the gas-phase diffraction data which yield a remarkably long P−F_{ax} bond.

Gas-Phase Structure of Me_4PF. The molecular structure of Me_4PF was determined by gas electron diffraction (GED) and predicted by theoretical calculations (Table 8). The radial distribution function (RDF) which was obtained by Fourier transformation of the experimental electron diffraction intensities is shown in Figure 7. The geometric parameters are listed in Table 9 together with those of known methylfluorophosphoranes.[49−51] Vibrational amplitudes are listed in Table 10 together with calculated values. During previous studies it was found that HF/6-31+G* calculations yield geometric parameters for methylfluorophosphoranes in excellent agreement with experimental data.[52,53] For Me_4PF the PF bond is overestimated with this method by 4.2 pm,

Table 9. Experimental Bond Lengths (pm) and Angles (°) of Methylfluorophosphoranes Me_nPF_{5-n} ($n = 0-4$)

	Me_4PF	Me_3PF_2 [a]	Me_2PF_3 [b]	$MePF_4$ [b]	PF_5 [c]
r(P−F_{ax})	175.3(6)	168.5(1)	164.3(3)	161.2(4)	157.7
r(P−F_{eq})			155.3(6)	154.3(4)	153.4
r(P−C_{eq})	182.6(4)	181.3(1)	179.8(4)	178.0(5)	
r(P−C_{ax})	188.4(8)				
r(C−H)	110.3(4)	111.4(6)	110.7(12)	109.9(31)	
∠(F_{ax}−P−C_{eq})	84.6(6)			88.2(4)	
∠(F_{ax}−P−F_{eq})			89.9(3)		90.0
∠(F_{eq}−P−C_{eq})			118.0(8)	122.2(9)	
∠(F_{eq}−P−F_{eq})					120.0

[a] From Ref. 49. [b] From Ref. 50. [c] From Ref. 51.

Table 10. Interatomic Distances, and Experimental and Calculated Vibrational Amplitudes for Gaseous Me_4PF (Without Nonbonded Distances Involving Hydrogen)[a]

	distance	ampl. (GED)	ampl. (B3LYP)
C−H	110	7.6(4)	7.6
P−F	175	5.6(4)	5.4
P−C_{eq}	183	5.4(4)[b]	5.2
P−Cax	188	5.8(4)[b]	5.6
F···C_{eq}	240	9.5 (10)	8.2
C_{ax}···C_{eq}	275	9.3(12)	8.5
C_{eq}···C_{eq}	315	11.7(12)	10.7
F···C_{ax}	363	7.5(18)	7.0

[a] Values in pm with 3σ uncertainties. [b] Difference to previous value set to calculated value.

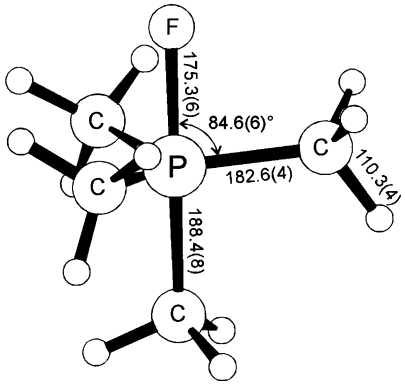

Figure 8. Gas-phase structure of Me_4PF.

thus we compared different theoretical methods (Table 8). Finally, the B3LYP/6-31G* method which reproduces the experimental bond lengths and angles as well as vibrational frequencies satisfactorily was chosen for deriving vibrational amplitudes from the calculated Cartesian force constants.

The GED intensities are reproduced very well with a trigonal bipyramidal structure of C_{3v} symmetry with one methyl group and the fluorine atom in axial positions. Structural models with equatorial position of the fluorine atom reproduce the experimental RDF poorly. This is in agreement with all quantum chemical calculations which predict trigonal bipyramidal structures with C_{3v} symmetry. The structure with equatorial position of the fluorine atom is predicted (B3LYP/6-31G*) to be higher in energy by 9.3 kcal/mol. According to the experimental analysis the equatorial P−C bond lengths of 182.6(4) pm in Me_4PF are slightly longer than those of Me_3PF_2 and are bent toward the fluorine atom with an F_{ax}−P−C_{eq} angle of 84.6(6)° (Figure 8). The methyl groups are arranged with one C−H bond parallel to

(49) Yow, H.; Bartell, L. S. *J. Mol. Struct.* **1973**, *15*, 209.
(50) Bartell, L. S.; Hansen, K. W. *Inorg. Chem.* **1965**, *4*, 1777.
(51) Hansen, K. W. *U.S. At. Energy Comm.* **1965**, IS-T-4.
(52) Kornath, A.; Neumann, F.; Ludwig, R. *Z. Anorg. Allg. Chem.* **2002**, *628*, 1835.
(53) Kornath, A.; Neumann, F.; Ludwig, R. *Z. Anorg. Allg. Chem.*, in press.

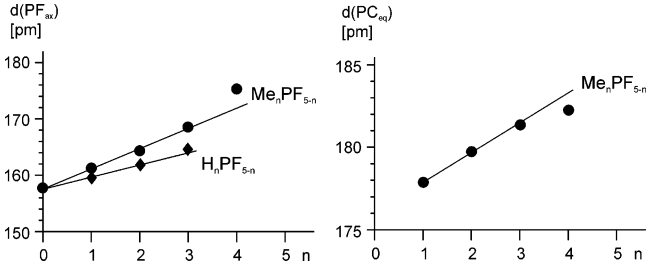

Figure 9. P−F_{ax} and P−C_{eq} bond distances in hydrido- and methylfluorophosphoranes.

the P−C_{ax} bond and a tilt of 4.8(22)° toward the P−F_{ax} bond. The molecule is the first example of a phosphorane with a methyl group in an axial position. The P−C_{ax} bond of 188.4(8) pm is longer than the P−C_{eq} bonds, revealing the different kinds of bonds in the molecule which can be rationalized in terms of semi-ionic, three-center four electron bonding for the axial ligands and mainly covalent P−C_{eq} bonds, respectively. The P−F_{ax} bond length of 175.3(6) pm is the longest P−F_{ax} bond observed in phosphoranes. Figure 9 shows that the stepwise substitution of a fluorine atom in the equatorial positions of PF_5 by a methyl group leads to a weakening of the P−F_{ax} and the P−C_{eq} bonds. This effect was explained by a repulsive interaction of the equatorial bonds with the lone pairs of the axial fluorine atoms.[54] For hydridofluorophosphoranes a similar trend is observed.[55,56] A substitution of one fluorine atom by a methyl group in the axial position causes a remarkable lengthening of the P−F_{ax} bond. Obviously, this substitution enhances the formation of semi-ionic, three-center four electron bonds, thereby causing the unusual length of the P−F_{ax} bond.

The exceptionally long PF bond of Me_4PF enables an easy formation of ionic $Me_4P^+F^-$ in the solid state, as well as in polar solvents, as shown in Figure 10. A lengthening of the PF bond combined with an umbrella motion of the equatorial

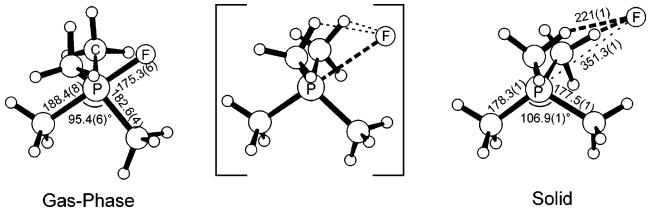

Figure 10. Transition between the molecular and ionic structure of Me_4PF.

methyl groups and their rotation approaches the bonding situation found in the crystal lattice. A similar mechanism with a fluorine atom dynamically moving within a solvate sphere can be considered to explain the missing fluorine couplings in the NMR spectra.

Conclusion

This study has shown that Me_4PF can serve as a source for "naked" fluoride. It possesses unique properties compared to other sources of naked fluoride. The salt is well soluble in acetonitrile and volatile in a vacuum. This may open new possibilities for the syntheses of novel compounds and applications for organic syntheses where highly concentrated solutions of anhydrous fluoride are required. Gaseous Me_4PF and solutions in nonpolar solvents have a phosphorane structure with an exceptionally weak P−F_{ax} bond. It is also the first example of a phosphorane with an axial methyl group.

Acknowledgment. This work has been supported by the Deutsche Forschungsgemeinschaft. We are grateful to Prof. Arne Haaland and Ing. Hans Vidar Volden, University of Oslo, Norway for the electron diffraction measurement.

Supporting Information Available: Tables listing crystal data and structure refinement, final atomic coordinates, hydrogen atom positions, final temperature factors, and bond distances (CIF and PDF). This material is available free of charge via the Internet at http://pubs.acs.org.

IC020663C

(54) Howell, M. *J. Am. Chem. Soc.* **1975**, *97*, 3930.
(55) Christen, D.; Kadel, J.; Liedtke, A.; Minkwitz, R.; Oberhammer, H. *J. Phys. Chem.* **1989**, *93*, 6672.
(56) Beckers, H.; Breidung, J.; Bürger, H.; Kuna, R.; Rahner, A.; Schneider, W.; Thiel, W. *J. Chem. Phys.* **1990**, *93*, 4603.